Control of an Induction Motor Using the Relay Method Approach

Iulia Inoan, Mihail Abrudean

*Automation Department, Technical University of Cluj-Napoca, 26-28 Baritiu Street, 400027, Cluj-Napoca.
E-mail: (iulia.inoan, mihai.abrudean)@aut.utcluj.ro*

Abstract: The authors approach by means of this paper an induction motor control for the rotation of a furnace hearth. The rotation regime of the rotary hearth furnace, used for heating up billets in order to prepare them for the rolling process, is jerky with stops at fixed angles. The hearth's rotation is carried out with two induction motors (IM) supplied by inverters and the rotation is measured with incremental encoders. In this paper the calculus of the rotation step, taking into account the billet's diameter, is carried out. Also the IM model is presented, the model in use is the fifth-order nonlinear model. Since the model is nonlinear the Ziegler-Nichols transient response method and the relay method is applied for the design of a PI motor speed's controller. Using the designed controller the motor speed is simulated and the number of revolutions made by the motor is calculated. The starting and stopping of the furnace hearth by using acceleration and braking ramps is ensured via simulation.

Keywords: Hearth rotation control, Induction motor, IM model, PI controller, Relay method, Ziegler-Nichols transient response method.

1. INTRODUCTION

Hot rolling process is the main procedure for obtaining seamless tube pipes. The hot rolling process technology involves several steps. The first step is to heat up the block of billets, previously cut at required lengths, from the ambient temperature to the rolling temperature, leading the material from the elastic domain to the plastic one. This basic step is done inside the rotary hearth furnace (Inoan, 2011).

The furnace used is CARUSEL type, with rotary hearth, and it has a continuous functioning in the technological flow of the rolling line. The furnace has five regulating temperature areas that have a total of 48 burners and consists of a sector for loading billets, two sectors for heating, a sector for preheating, and a sector for unloading billets (Muresan, 2010). For the supply and evacuation of the blocks, the furnace is equipped with a loading machine and one for unloading. The furnace also has an inactive area from thermal point of view (Muresan, 2011a).

The furnace's hearth is rotated by two action mechanisms that are placed in reverse direction, at the exterior of the furnace. The rotation regime of the hearth is jerky, with stops at fixed or continuous angles. In the periods when the hearth stops the loading and unloading machines supply and respectively evacuate the blocks of billets from inside the furnace (Inoan, 2012). The loading-unloading doors can be manipulated in the loading-unloading rhythm, and are being activated with electromagnetic hoists. At high rolling rhythms, of 4 pieces/minute, they have to be always open. The doors are closed only when the rolling process stops.

The billet's loading on to the hearth is being done uniformly on the entire sitting circle. In order to ensure the entrance of the loading or unloading clipper's jaws, and also for an optimum heating of the billets, a minimum distance between two neighboring billets, measured on the sitting circle, is left. This distance equals at least with the diameter of the billet and will not be below 100 mm (Muresan, 2009).

2. PROBLEM STATEMENT

Currently all the above described operations represent a full cycle of loading and unloading and are done manually, since the mounted furnace control system failed to ensure the performances accuracy needed.

Given the fact that actuators are physically worn due to repeated winding, and the fact that the pearling of contactors engines drive's contacts often lead to stops, replacing the engines and the drive system is impetuous necessary. Also for a precise control of the hearth's rotation step a modern drive is required, in order to meet high precision requirements. Thus, a noiseless start and stop of the furnace hearth by using acceleration and braking ramps is ensured.

In this paper the authors propose that the hearth's rotation to be carried out by two Alternating Current (AC) servo motors supplied by inverters, and the rotation to be measured with incremental encoders. Thus a servo motor that has an encoder of 11 bits and incorporated brake was chosen. The AC motor's nominal operating parameters are detailed bellow in Table 1.

Both acceleration and braking ramps can take various values. Therefore an engine can be turned on or off in one or more steps. The value entered for the ramp will reflect how steep is the slope and what will be the time in which the engine starts or stops.

The current speed of the motor in use is 750 rpm, but the new motor due to the usage of ramps and high performance can run at a speed of 850 rpm.

Table 1. IM nominal operating parameters.

Parameter	Value	Unit
Rated speed (n^n)	2960	Rpm
Nominal power (P^n)	37	KW
Nominal torque (τ^n)	177	Nm
Nominal current (I_n)	70	A
Rated voltage (U_n)	412	V
Power factor ($cos\varphi$)	0,85	
Magnetizing current (I_μ)	29	A
Efficiency (μ^n)	0,912	
Rated frequency (f_n)	50	Hz
Moment of inertia (J)	0.49	Kg·m^2
Mass (m)	175	Kg

3. DESCRIBING THE FURNACE HEARTH ROTATION

3.1 The rotation acting mechanism

Under the metal frame that supports the furnace's hearth sits a rack with 597 teeth, with a width of 300 mm, used for the rotation of the hearth. The toothed rim has 34 sectors of 10° 15'14'' each, and a sector of 11° 29'26''. The internal diameter of the rim is 11640 mm at the center of the furnace and 11940 mm at the exterior of the furnace (Muresan, 2008).

The rim conjugates with two pinions of 17 teeth each, placed at opposite direction. The two pinions are activated by three steps reducers with a gear ratio of i_R=291.864, by two electric motors. The two electric motors are in fact induction motors (IM) with coiled rotor, each one having the power of 37 KW (see Table 1).

The command of the motors is being done manually by an operator with the help of a command key. The acting system is reversible, meaning that the hearth can be rotated in both directions. The total gear ratio from the engine to the toothed rim is equal with the product between the gear ratio of the reducer (i_R) and the pinion-rim gear ratio (i_{CDP}):

$$i_T = i_R \cdot i_{CDP} = 291.864 \cdot 35.12 = 10249 \qquad (1)$$

Thus, for a complete rotation of the furnace's hearth the engine's shaft performs 10249 rotations (rot).

In order to heat a previously loaded billet the hearth makes a rotation of 336°, since the area between the loading and the unloading machine of 24° is a no billets area.

This implies that in order to unload a billet from inside the furnace the motor must perform a number of turns equal to:

$$\frac{336°}{360°} \cdot i_T = \frac{336°}{360°} \cdot 10249 = 9566 \qquad (2)$$

3.2 The calculus of the rotating step

In practice only two different diameters are used for billets: 150 mm and 180 mm, thus being necessary and sufficient to calculate two different rotation steps for the hearth (Muresan, 2008).

The average diameter of the hearth is D =19700 mm, and the length of the corresponding circle is:

$$L_{dm} = \pi \cdot D = 61889.37 \text{ mm} \qquad (3)$$

The active hearth's segment is

$$x = \frac{336°}{360°} 2\pi \qquad (4)$$

Thus the useful circle's length is:

$$L = x \cdot \frac{D}{2} = 57763.41 \text{ mm} \qquad (5)$$

In the following, the maximum number of billets that can be charged inside the furnace, and also the value of the rotation step, is calculated.

The billets number is obtained by dividing the useful circle's length at twice the diameter of the billet. The rotation step is calculated by dividing the useful portion of the hearth in degrees at the maximum number of billets that fit inside de furnace (Muresan, 2008).

Thus for a diameter of 150 mm a number of 192 billets and a rotation step of 1.75 degrees resulted, as for a diameter of 180 mm a maximum number of 160 billets at a rotation step of 2.1 degrees resulted.

Further work will treat the case of a 150 mm in diameter billet.

The number of rotation (n_1) needed to complete a rotation step is determined by knowing that for a useful circle's rotation of 336° the AC motor must generate 9566 rpm.

$$n_1 = \frac{9566 \cdot 1,75^0}{336^0} = 49.82 \text{ rot} \qquad (6)$$

The number of pulses generated by the encoder when it is placed on the motor's shaft is given below.

$$2048 \cdot n_1 = 102040 \text{ pulses} \qquad (7)$$

In the embodiment in which the encoder is placed at the exit of the reducer, it generates:

$$\frac{2048 \cdot n_1}{i_R} = \frac{2048 \cdot n_1}{291,864} = 349 \text{ pulses} \qquad (8)$$

The number of pulses will be processed by the PLC ant it will stop the hearth after the encoder generates the required number of pulses corresponding to a rotation step.

The braking ramp's time can be calculated so that the brake system is optimal, but also to cover the losses of pulses from different causes. For example at every one thousand pulses numbered one is lost, and the software solution to this problem is complicated. Instead these impulses can be

covered during braking, thus, eliminating all errors of measurement or processing.

If the encoder is placed at the exit of the reducer then counting is simpler due to the fact that far fewer pulses are emitted, but in this case another encoder is necessary.

4. MODEL OF THE INDUCTION MOTOR

4.1 The mathematical model

The nonlinear mathematical model used in this paper is the fifth-order model that gives the dynamics of an induction motor with one pole pair in a fixed frame a - b attached to stator (Yazdanpanah, 2008). The model is defined by the following equations (Aurora, 2005):

$$\frac{d\psi_a}{dt} = -\alpha\psi_a - \omega\psi_b + L_M\alpha i_a$$

$$\frac{d\psi_b}{dt} = -\alpha\psi_b - \omega\psi_b + L_M\alpha i_a$$

$$\frac{di_a}{dt} = -\beta\frac{d\psi_a}{dt} + \frac{1}{\gamma L_s}(u_a - R_s i_a)$$ (9)

$$\frac{di_b}{dt} = -\beta\frac{d\psi_b}{dt} + \frac{1}{\gamma L_s}(u_b - R_s i_b)$$

$$\frac{d\omega}{dt} = \frac{1}{J}\frac{L_M}{L_r}(\psi_a i_b - \psi_b i_a) - \frac{K_f}{J}\omega - \frac{M_R}{J}$$

In which the state variables are: the rotor speed ω, the rotor fluxes (ψ_a, ψ_b) and the stator currents (i_a, i_b). The stator voltages (u_a, u_b) constitute the control signals. L_M represents the mutual inductance, (L_s, L_r) are the stator and the rotor inductances, (R_s, R_r) are the stator and the rotor windings resistances, J is the moment of inertia, K_f is the friction coefficient and M_R is the load torque. For concision the following notation were used:

$$\alpha = \frac{R_r}{L_r}; \; \beta = \frac{1}{\gamma}\frac{L_M}{L_s L_r}; \; \gamma = 1 - \frac{L_M^2}{L_s L_r}.$$ (10)

Phase transformation of the model from the a-b reference system was not addressed in the paper, but in actual operation it is required to be performed (Etien, 2013).

4.2 The induction motor

The rotary hearth induction motor has one pair of stator poles and it is designed at a nominal power of 37kW, a rated speed of 2940 rev/min, respectively a nominal frequency of 50 Hz (Table 1). The constants used in (9) are as follows: $J = 0.4$ Kg·m^2, $K_f = 0.1115$, $R_r = 0.156 \ \Omega$, $R_s = 0.294 \ \Omega$, $L_r = 0.0417$ H, $L_s = 0.0424$ H, $L_M = 0.041$ H. The values of α, β and γ coefficients from the IM model result immediate using the values and the motor parameters previously described.

4.3 Model validation

In order to validate the model the simulation scheme for the engine speed given in Fig. 1 is implemented in Matlab® Simulink. The induction motor is considered to be an open loop process (Colosi, 2013).
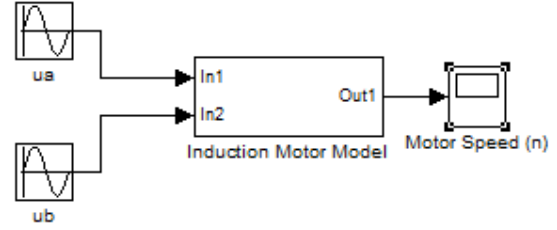

Fig. 1. Simulation diagram for the induction motor speed.

The nonlinear model of the motor is implemented in the subsystem Induction Motor Model (Muresan, 2011b). The output of the system (see Fig. 2) is considered to be the motor speed (n), which is proportional to the angular velocity (ω) and results using (11):
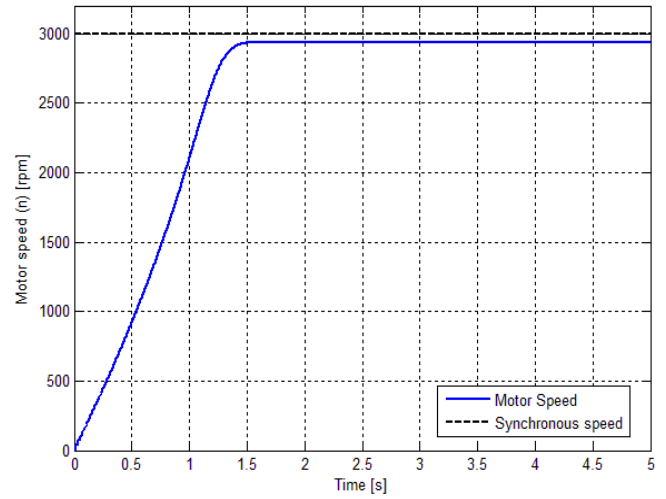
$$n = \frac{30}{\pi} \cdot \omega$$ (11)

Fig. 2. The open loop motor speed.

The figure above aims to simulate the nominal value of the corresponding motor speed (n_n=2940 rpm). To obtain the rated speed it is required to use the input signals (stator voltages u_a and u_b) given in (12) and (13) where $f_n = 50$ Hz is the nominal frequency of the power supply.

$$u_a = 220\sqrt{2} \cdot \sin(2\pi f_n t + \frac{\pi}{2})$$ (12)

$$u_b = 220\sqrt{2} \cdot \sin(2\pi f_n t)$$ (13)

It can be seen that the response of the system is stabilized at the value n=2940 rpm. The rotational speed of the rotating magnetic field is given by (Neamtu, 2007):

$$n_0 = \frac{60 f_n}{p}$$ (14)

where p is the number of poles pairs of the motor stator. In the considered system $p = 1$, thus $n_0 = 3000$ rpm.

Fig. 2 highlights the fact that the closed loop system response does not reach the steady state value of 3000 rpm, i.e. the synchronous speed. This is due to the induction motor sliding, which is defined by the relation (Campeanu, 1996):

$$s = \frac{n_0 - n_n}{n_0} = \frac{3000 - 2940}{3000} = 0.02 \qquad (15)$$

5. INDUCTION MOTOR CONTROL

An automatic motor control implies the possibility of changing its value according to the technological requirements imposed, and the opportunity to reject the effect of disturbances (Abrudean, 1998). The authors use for designing the motor speed controller experimental approaches, in order to obtain PID controllers.

These methods are used as the model describing the operation of the induction motor is nonlinear (Zarnescu, 1999).

5.1 Ziegler-Nichols transient response method

The first method applied by the authors is the Ziegler-Nichols transient response method, also known as the open-loop method. A step input signal is applied to the controlled process and the process output is recorded and analyzed. This method can be applied to all systems that have a critically damped or overdamped character (Ogata, 2009).

From the recorded step response the open-loop gain (k_f), the loop apparent deadtime (τ), and the loop time constant (T) are determined by drawing a tangent line at the inflection point of the step response's curve. The open-loop gain is obtained as the ratio between the steady state value of the process output signal (y_{ss}) and the steady state value of the input signal (u_{ss}).

$$k_f = \frac{y_{ss}}{u_{ss}} \qquad (16)$$

The deadtime represents the difference between the intersection of the tangent line with the time axis, and the time at which the input signal starts. The time at which the tangent line intersects with the steady state value represent the sum of the loop apparent deadtime and the loop time constant. Thus, the two values are read directly from the plot.

In order to design a PID controller Ziegler and Nichols suggested to use the formula presented in Table 2 to determine the values for the proportional gain k_p, the integral time T_i and the derivative time T_d, based on the parameters described above.

Table 2. Ziegler-Nichols formula for the open-loop method.

Controller type	The gain	The integral time	The derivative time
P	$\dfrac{T}{\tau}$	∞	—
PI	$\dfrac{0.9T}{\tau}$	$\dfrac{\tau}{0.3}$	—
PID	$\dfrac{1.2T}{\tau}$	2τ	0.5τ

5.2 The relay method

Below the authors present a method for designing the motor speed controller using the relay method. This method is based on a changeover relay, with or without hysteresis, placed on the controlled process direct path (see Fig. 3) and consists in bringing the system at its stability limit, obtaining sustained oscillations at the output (Dobra, 1999).
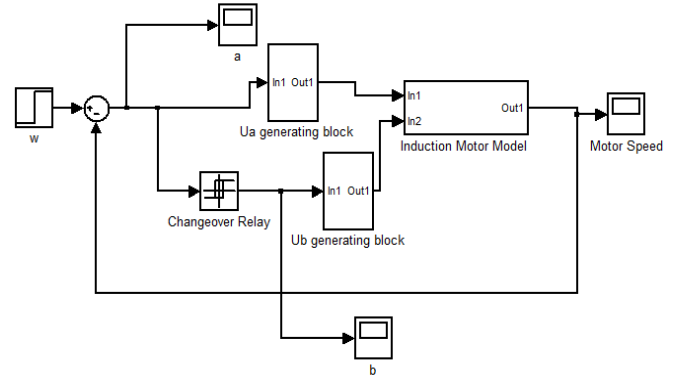

Fig. 3. Relay method diagram applied to the induction motor.

From the output signal's graph the values of the critical period (T_0) and the oscillation amplitude (A_0) are read (Duma, 2011). Knowing this value one can calculate the changeover relay's ultimate gain (K_0) by using the following formula:

$$K_0 = \frac{4b}{\pi A_0} \qquad (17)$$

Given the values of K_0 and T_0 the parameters of PID controller result immediately by applying Ziegler-Nichols formula given in Table 3 (Dobra, 1999).

Table 3. Ziegler-Nichols formula for the relay method.

Controller type	The gain	The integral time	The derivative time
P	$0.5 \cdot K_0$	∞	—
PI	$0.45 \cdot K_0$	$0.8 \cdot T_0$	—
PID	$0.6 \cdot K_0$	$0.5 \cdot T_0$	$0.12 \cdot T_0$

5.3 The induction motor control

First the Ziegler Nichols open-loop method is applied. The open-loop structure is implemented in Simulink MATLAB® and a step signal of 800 is set as the input signal for the induction motor's speed. Thus, the step response depicted in Fig. 4 is obtained. The deadtime and the time constant are read directly from the plot and the open-loop gain is being calculated. The corresponding values are given below.

$$\tau = 0.01 \; s \qquad (18)$$

$$T = 3.75 \; s \qquad (19)$$

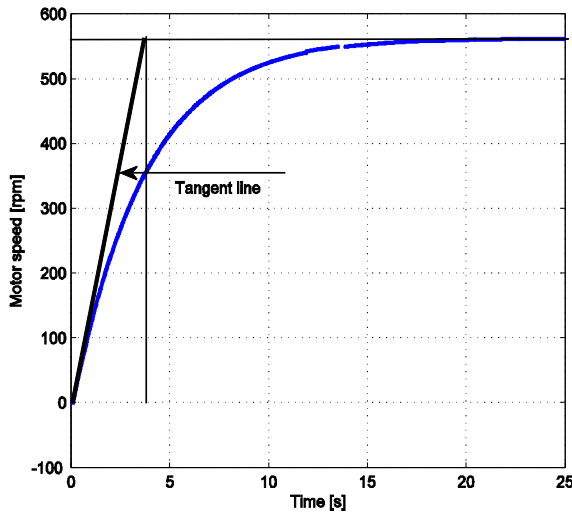$$k_f = \frac{564}{800} = 0.705 \qquad (20)$$

Fig. 4. The open-loop step response for the induction motor's speed.

Replacing the values from (18), (19) and (20) in Table 2 formulas the authors obtain a PI controller, having the transfer function given in (21).

$$H_{R_1}(s) = K_{P_1}\left(1 + \frac{1}{T_{I_1}s}\right) = 337.5\left(1 + \frac{1}{0.0333s}\right) \qquad (21)$$

Second the relay method is applied for the design of another PI motor speed's controller. Fig. 3 illustrates the structure implemented in Simulink MATLAB® in order to bring the motor speed to a sustained oscillating form (Muresan, 2011b). In this structure the reference signal value is set to zero, the exit value of the changeover relay is $b = \pm 1$ and the hysteresis value is $a = \pm 50$.

The blocks generating the two supply voltages implement the appropriate waveforms and receive as input the sinusoidal signal u_a described in (12) and the sinusoidal signal u_b described in (22).

$$u_b = b \cdot 220\sqrt{2} \cdot \sin(2\pi f_n t) \qquad (22)$$

As for the voltage sine-waves the sign "-"or "+" means phasing them in a sense or in the other by π radians. In order to obtain maintained oscillations it is necessary that only one of the two voltages to be out of phase, in this case u_b. If both voltages would be out of phase simultaneously then the maintained oscillatory regime would not be possible.

The authors use two simplifying assumptions namely the transducer and actuator are considered non-inertial and the transducer's gain is equal to one.

Shortly after the beginning of the simulation one can observe the speed oscillation maintenance (see Fig. 5). Negative speeds correspond to a rotation of the rotor motor in reverse.

From the detailed graph, given in Fig. 6, the parameters of interest are read and the values, along with the changeover relay's ultimate gain value, are given in (23).
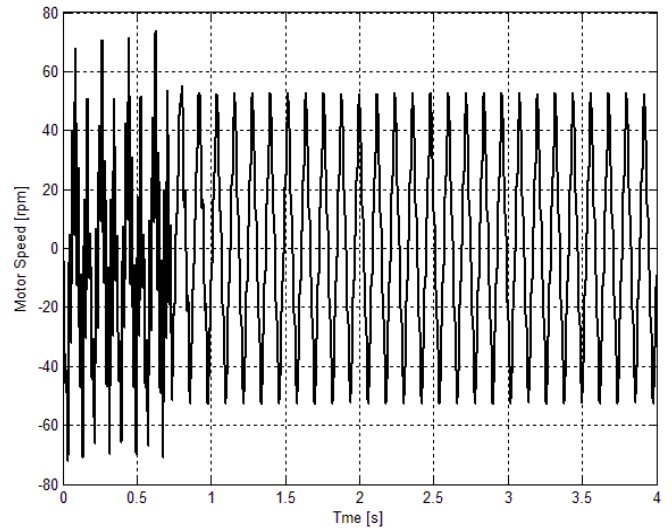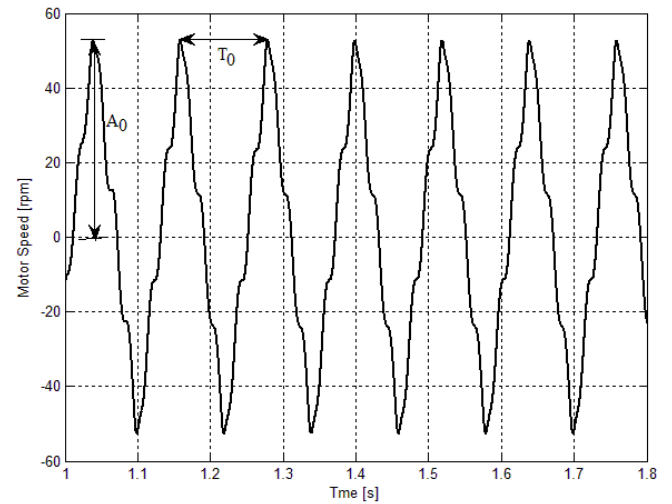

Fig. 5. Motor's speed maintained oscillations.

Fig. 6. Detailed view of the motor's speed maintained oscillations.

$$A_0 = 52.6 rot / \min$$
$$T_0 = 0.12s \qquad (23)$$
$$K_0 = 0.0242$$

Using the above presented values and the data in Table 3 the authors obtain a PI controller with the parameters and transfer function given in (24).

$$H_{R_2}(s) = K_{P_2}\left(1 + \frac{1}{T_{I2}s}\right) = 0.0109\left(1 + \frac{1}{0.096s}\right) \qquad (24)$$

Fig. 7 shows the simulated controlled motor's speed obtained when using the H_{R1} and the H_{R2} designed controllers. It can be seen that the H_{R1} control structure is the fastest one but it exhibits the highest overshoot. Also when using this control structure a ringing effect occurs in the control signal, thus, the controller obtained by means of the relay method is first chosen. This controller has an overshoot of 31.75%.
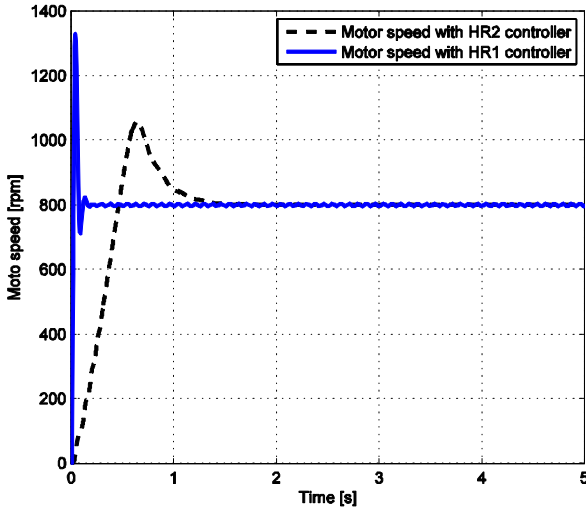
Fig. 7. Comparison between the two designed PI controllers for the induction motor speed control.

Since from the performed simulations for the closed-loop motor control system it was observed that the relay method controller requires some improvements, meaning no overshoot, the authors chose another controller. The new controller is obtained by changing the controller's gain until the overshoot for the induction motor's speed is eliminated. This produced a new controller that has the following transfer function. This controller will be further use.

$$H_{R_3}(s) = K_{P_3}\left(1 + \frac{1}{T_{I_3}s}\right) = 0.0027\left(1 + \frac{1}{0.096s}\right) \qquad (25)$$

6. SIMULATION RESULTS

6.1 The induction motor's speed simulation

The testing of the control system is done by means of simulation as access to the industrial equipment was not possible. Implementation and validation of control structures can only be done in stages of furnace intervention, when there is a state of emergency break and the furnace is out of order. This because each prolonged stop of the furnace represent a break in the production workflow. As future work the authors wish to obtain the experimental results necessary for the validation of the proposed control structure.

The simulation diagram used for the induction motor's speed control system is shown in Fig. 8, this being the structure implemented in Simulink MATLAB®.

In Fig. 8 the output signal from the controller represents the frequency of the supply voltage. The supply is performed by means of two VCO blocks which affect depending on the value of the input signal the frequency of the sine wave generated by each unit separately. The other parameters of the power signals are set inside the two blocks.
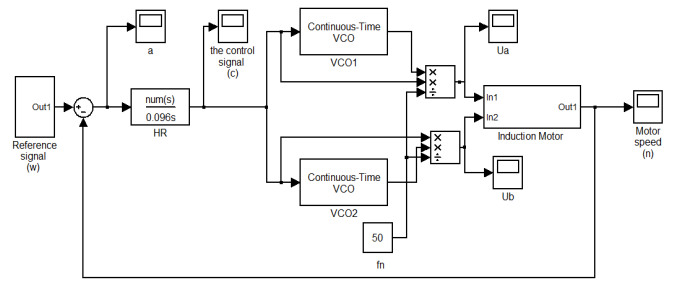

Fig. 8. Induction motor's speed control system diagram.

To maintain a constant value of the amplitude of the magnetic flux it is necessary to maintain a constant ratio *u/f*. Thus the values of the signals generated by VCO blocks are processed and the following supply voltages result:

$$\begin{aligned} u_a &= \frac{u_1 \cdot f}{f_n} \\ u_b &= \frac{u_2 \cdot f}{f_n} \end{aligned} \qquad (26)$$

The implementation of (26) was carried out in a simplified manner in order to carry out the simulations. In fact, in order to maintain a constant amplitude value of the magnetic flux a separate controller is needed.

Since the model is nonlinear, the motor speed does not follow a perfect ramp thus the authors propose the following solution in order to obtain a response, for the motor's acceleration and braking, as close as possible to that of a ramp (see Fig. 10).

The proposed solution consists in a reference signal composed by a sequence of ramps and steps of different values, as shown in Fig. 9.
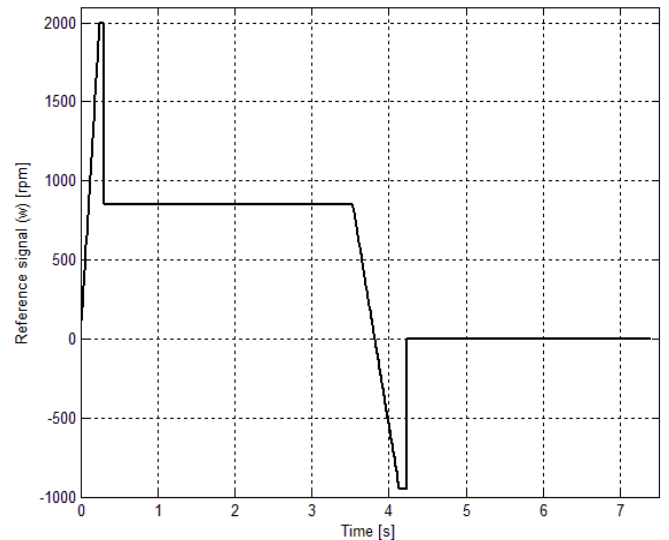

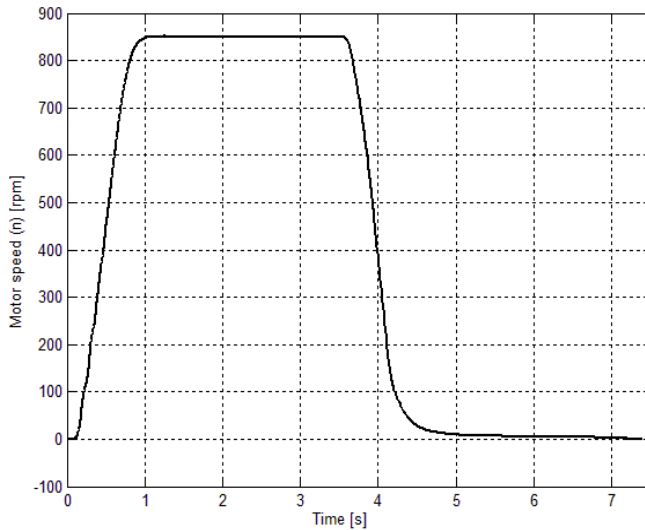Fig. 9. The reference signal for the motor's speed control system.
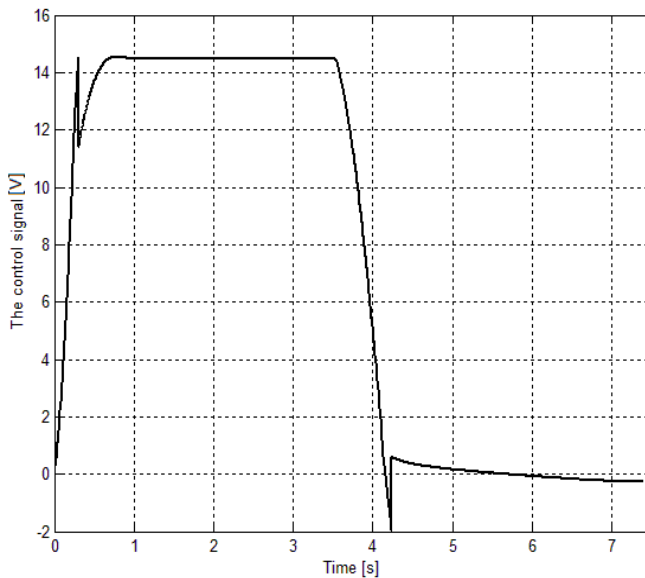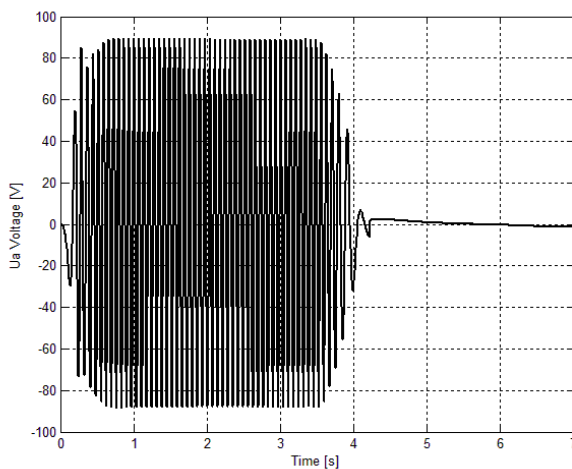
Fig. 10. The induction motor's speed.

Fig. 11. The control signal generated by the controller.

Fig. 12. The supply voltage signal u_a time evolution.

The time evolution of the control signal generated by the controller is depicted in Fig. 11. This signal is processed and transmitted as the supply voltage frequency that stabilizes the corresponding values to maintain the motor speed reference value.

For a better understanding of the effect of applying a constant ratio of voltage and frequency, Fig. 12 shows the evolution of the supply voltage signal u_a.

6.2 The calculation of the induction motor's rotations

The calculation of the induction motor's rotations is carried out due to the fact that in order for the furnace hearth to do a complete rotation step a certain amount of rotations are necessary. The authors verify whether the proposed control system generates the necessary rotations for a billet diameter of 150 mm given in (6).

In order to calculate the number of revolutions made by the motor the authors have divided the motor's speed curve given in Fig. 10 in several sections. The sections corresponding to starting and stopping the motor from the chart are mainly approximated by ramps. The graph's sections that do not fit on the main ramp are approximated by a polynomial function.

The average speed (*n*) of each section is calculated and the number of revolutions (*rev*) results from the following formula:

$$rev = \frac{n \cdot t}{60} \text{ rot} \tag{27}$$
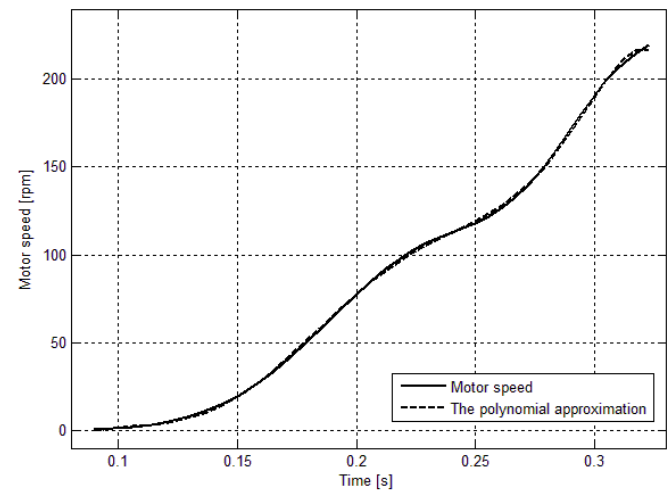
where *t* represents the section time.

Fig. 13. The first section from the motor speed curve and the polynomial approximation.

The first section of the graph corresponds to the selection between t_1=0.0897 s and t_2=0.3232 s. This section is approximated by the polynomial function (P_1), and from Fig. 13 one can observe that the motor speed and the polynomial approximation for the specified section are superimposed.

$$P_1(t) = -4.0514 \cdot 10^8 t^7 + 5.145 \cdot 10^8 t^6 - 2.6599 \cdot 10^8 t^5 +$$
$$+7.2037 \cdot 10^7 t^4 - 1.0971 \cdot 10^7 t^3 + 9.3932 \cdot 10^5 t^2 - 4.1797 \cdot \quad (28)$$
$$\cdot 10^4 t + 741.1472$$

In order to determine the number of motor's revolutions on this section it is necessary to know the average speed of the motor, determined using the following formula:

$$n_{med} = \frac{1}{t_2 - t_1} \cdot \int_{t_1}^{t_2} P(t)dt = \frac{19.9808}{0.2335} = 85.57 \text{ rpm} \quad (29)$$

The number of revolutions for the first section is obtained as follows:

$$rev_1 = \frac{n_{med} \cdot (t_2 - t_1)}{60} = 0.33 \text{ rot} \quad (30)$$

The second section of the motor's speed corresponds to the selection between $t_2 = 0.3232$ s and $t_3 = 0.6964$ s. This portion can be approximated by a ramp, as can be seen from Fig. 14. Thus, the motor's average speed and the number of revolution on this area are:

$$n_{med2} = 219,7031 + \frac{703.6078 - 219,7031}{2} = 461.655 \text{ rpm} \quad (31)$$

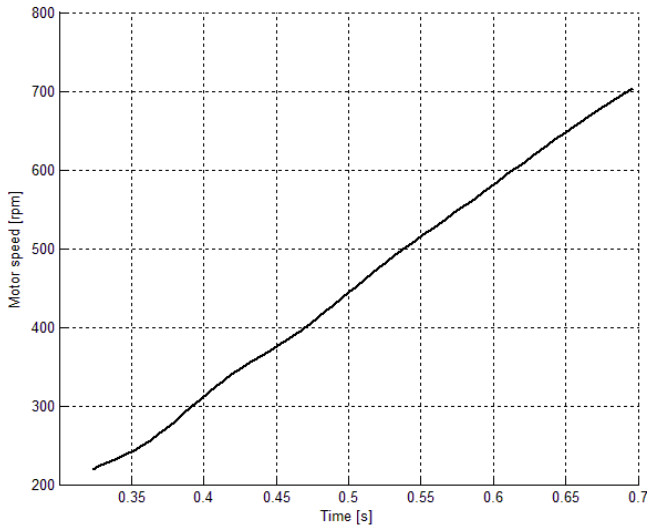$$rev_2 = \frac{n_{med2} \cdot (t_3 - t_2)}{60} = 2.87 \text{ rot} \quad (32)$$

Fig. 14. The second section from the motor speed curve.

The third section corresponds to the selection between $t_3 = 0.06964$ s and $t_4 = 1.0866$ s. This section is also approximated by a polynomial function (P_3). In Fig. 15 the motor speed and the polynomial approximation for this section are depicted.

$$P_3(t) = -46902t^5 + 212910t^4 - 3812 \cdot 10^2 t^3 + 334910t^2 - \quad (33)$$
$$-1433 \cdot 10^2 t + 24426$$

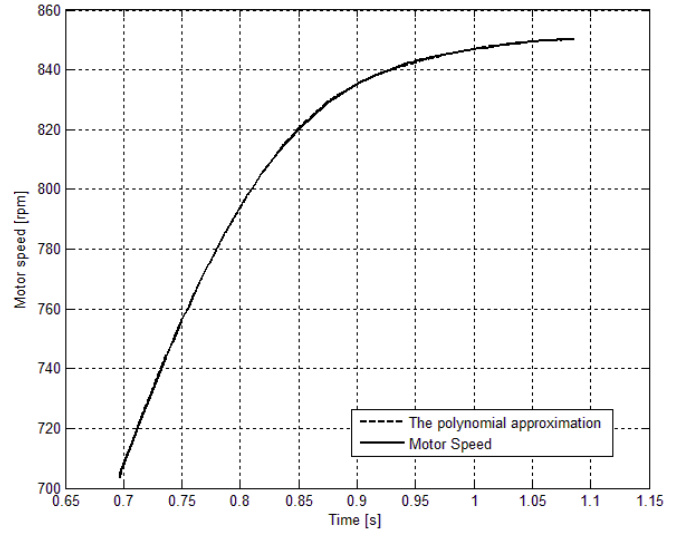The average speed of the motor is 813.8631 rpm, determined using (29).

Fig. 15. The third section from the motor speed curve and the polynomial approximation.

The number of revolutions for the third section is:

$$rev_3 = \frac{n_{med3} \cdot (t_4 - t_3)}{60} = 5.29 \text{ rot} \quad (34)$$

The fourth section is represented by the motor's speed from $t_4 = 1.0866$ s and $t_5 = 3.5095$ s. Analyzing the motor's speed, given in Fig. 10, the average speed is determined as 850 rpm, since on this section the speed is constant. The corresponding number of revolution for this average speed is:

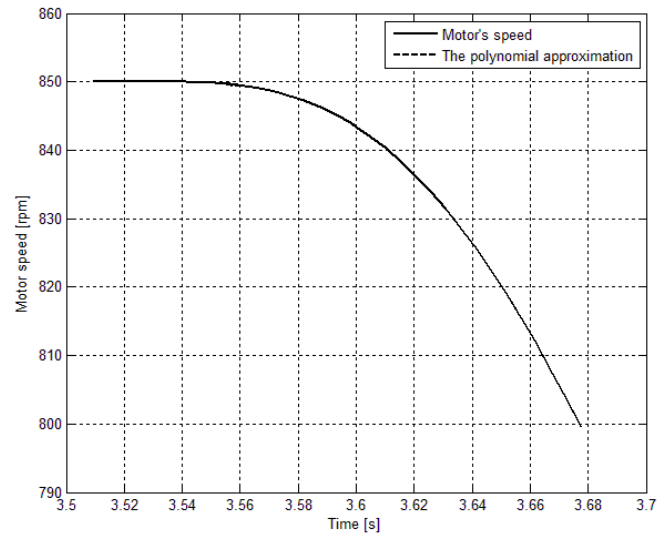$$rev_4 = \frac{n_{med4} \cdot (t_5 - t_4)}{60} = 34.32 \text{ rot} \quad (35)$$

Fig. 16. The fifth section from the motor speed curve and the polynomial approximation.

The section between $t_5 = 3.5095$ s and $t_6 = 3.6776$ s represents the fifth section chosen, shown in Fig. 16. This section is approximated by the following polynomial function:

$$P_5(t) = -3.2466 \cdot 10^6 t^7 + 8.0643 \cdot 10^7 t^6 - 8.5802 \cdot 10^8 t^5 +$$
$$+5.069 \cdot 10^9 t^4 - 1.7958 \cdot 10^{10} t^3 + 3.8153 \cdot 10^{10} t^2 - 4.5007 \cdot \quad (36)$$
$$\cdot 10^{10} t + 2.2741 \cdot 10^{10}$$

When using a polynomial approximation of the speed curve the number of revolutions can be obtained using the following formula:

$$rev = \frac{\int_{t_1}^{t_2} P(t) dt}{60} \text{ rot} \quad (37)$$

Thus the number of revolutions for the fifth section is 2.34 rot.

The sixth section is considered to be a ramp, and it represents the section between t_6=3.6776 s and t_7=3.9315 s (see Fig. 10). The average motor's speed is 648.95 rpm and the revolution numbers is obtained as 2.74 rot.

The next section is also approximated by a ramp, and is the speed curve between t_7=3.9315 s and t_8=4.2137 s (see Fig. 10). On this section the average speed is calculated as 298.32 rpm having a corresponding revolution number of 1.40 rot.

The last portion of the graph, between times t_8=4.2137 s and t_9=7.3193 s, does not correspond to a ramp thus another polynomial approximation is needed. The identified polynomial function is given below as P_8, and the graphic representation of the motor's speed and the motor's speed approximation are given in Fig. 17.

$$P_8(t) = -4.2538t^7 + 178.1841t^6 - 3186.5t^5 + 31535t^4 -$$
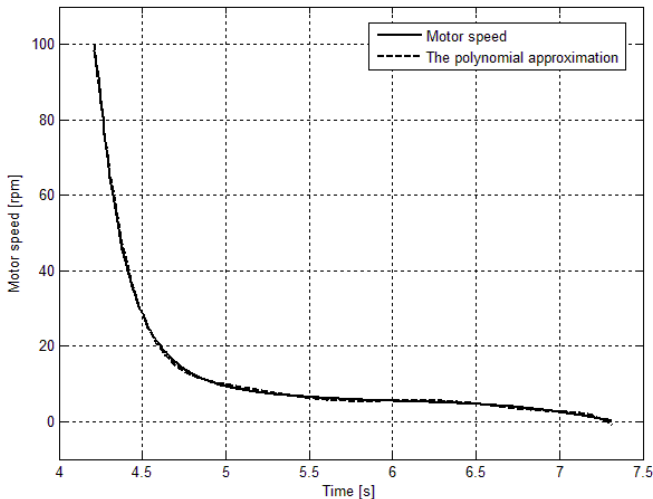$$-186530t^3 + 659460t^2 - 12904 \cdot 10^2 t + 10781 \cdot 10^2 \quad (38)$$

Fig. 17. The last section from the motor speed curve and the polynomial approximation.

Using (37) the revolution number for the last section is obtained as 0.59 rot.

The total number of revolution for the acceleration and braking of the motor is:

$$rev_{tot} = \sum_{i=1}^{8} rev_i = 49.82 \text{ rot} \quad (39)$$

The number above corresponds to the number of rotation (n_1) needed in order to complete a step in the rotation of the rotary hearth given in (6) for a billet diameter of 150 mm.

7. CONCLUSIONS

In this paper the authors present a control of an induction motor using a controller tuned using the relay method and the Ziegler-Nichols transient response method. In order to comply with the hearth's rotation step, and in order to achieve proper loading and unloading of billets, a control system is required for the motor used to rotate the furnace hearth. To design the required controller the relay method and the Ziegler-Nichols transient response method was applied since the model of the induction motor is nonlinear. The obtained controllers are compared based on their overall performance. A controller most suitable for the induction motor's speed control was chosen.

The possibility of using acceleration and braking ramps for the motor resulted via simulation.

By implementing the control structure presented in this paper the possibility of using an automated loading and unloading billets system is created, by automating the jerky rotation of the hearth. The current rolling rate is 3.5 units per hour and is given by the number of billets coming out of the furnace. By increasing the speed of the motors that move the hearth one can increase the rolling rate to 4-5 units/hour, which would lead to increased productivity.

REFERENCES

Abrudean, M. (1998), Systems Theory and Automatic Control, *Mediamira Publisher*, Cluj-Napoca.

Aurora, C. and Ferrara A., (2005), Sensorless speed and flux regulation of induction motors: a sliding mode approach. *Proceedings of 16th IFAC World Congress*. Prague.

Campeanu, A., Iancu, V. and Other (1996), Electric drive machines, *Scrisul Romanesc Publisher*, Craiova.

Colosi, T., Unguresan, M.L. and Other (2013), Numerical simulation of distributed parameter processes, *Springer Heidelberg Publisher*, New York Dordrecht London.

Dobra, P. (1999), Nonlinear systems, *UTPress Publisher*, Cluj-Napoca.

Duma, R., Trusca, M. and Other (2011), Tuning and implementation of PID controllers using rapid control prototyping, *CEAI, Vol. 13, No. 4*, pp. 64-73.

Etien, E. (2012), Modeling and simulation of soft sensor design for real-time speed estimation, measurement and control of induction motor, *ISA Transactions*, In press.

Inoan, I., and Abrudean, M. (2011), Signal recovery from the time evolution graph using image processing techniques, *Automation Computers Applied Mathematics*, vol. 20, Mediamira Science Publisher, pp. 185-190.

Inoan, I., Dumitrache, D.C. and Other (2012) A control system design for the positioning system for a billets unloading machine, *Proceedings of 2012 IEEE*

International Conference on Automation, Quality and Testind, Robotics, Cluj-Napoca.

Muresan, V. and Abrudean, M. (2008). The Control of the step for the furnace with rotary hearth in the technologic flow for manufacturing pipes without welding, *IEEE International Conference on Automation, Quality and Testing, Robotics Proceedings*, Cluj-Napoca, pp.258-261.

Muresan, V. and Abrudean, M. (2009). Control System Optimization of Rotary Hearth Furnace Charging / Discharging. *5th International Symposium on Applied Computational Intelligence and Informatics Proceedings*, Timisoara, pp. 277-282.

Muresan, V. (2010). Mathematical modelling and numerical simulation of the temperature control system in a furnace with rotary hearth. *IEEE International Joint Conferences on Computational Cybernetics and Technical Informatics Proceedings,* Timisoara, pp. 203-208.

Muresan, V., (2011a). Numerical simulation of the temperature in a rotary hearth furnace, using Taylor Serie. *Scientific bulletin of "Politehnica"University from Timisoara Vol. 56(70),* Politehnica Publisher, Timisoara, pp. 65-74.

Muresan, V., (2011b). Industrial processes control. Laboratory use, *UTPress Publisher*, Cluj-Napoca.

Neamtu, V. (2007) *Electrical Machines*, MediamirPublisher, Cluj-Napoca.

Ogata, K. (2009) *Modern Control Engineering - Fifth edition*, Prentice Hall.

Yazdanpanah, R., Soltani, J. and Other, (2008) Nonlinear torque and stator flux controller for induction motor drive based on adaptive input-output feedback linearization and sliding mode control, *Energy Conversion and Management,* Vol. 49, pp. 541-550.

Zarnescu, H., (1999) *Automatic control Engineering II. The design of automatic control systems*, page 263 – 268, Targu Mures